DEPINNING AND MOTION OF CRYSTAL DISLOCATIONS

L.L. Bonilla[1], *A. Carpio*[2]

[1] G. Millán Institute of Modeling, Simulation and Industrial Mathematics, Universidad Carlos III de Madrid, 28911 Leganés, Spain

[2] Departamento de Matemática Aplicada, Universidad Complutense de Madrid, 28040 Madrid, Spain

bonilla@ing.uc3m.es, ana_carpio@mat.ucm.es

ABSTRACT: We present a discrete model of dislocations for cubic crystals that describes the core of dislocations and it approaches the correct equations of anisotropic elasticity in the far field of defects. We analyze the depinning of dislocations near the Peierls stress and show that this transition can be understood as a global bifurcation whose character depends on the underlying dynamics.

Keywords: Discrete dislocation models, traveling waves, Peierls stress, edge dislocation depinning

1 INTRODUCTION

Discrete models of dislocations have been analyzed since Frenkel and Kontorova (FK) studied a model of interconnected harmonic springs in a periodic potential [1]. In this and related models, the distortion decays exponentially fast far from the core of a dislocation unlike the algebraic decay in elasticity [2]. Other discrete models modify the FK model so as to achieve algebraic decay of the distortion far from dislocation cores. Examples are Suzuki's modeling of moving screw dislocations in terms of sliding chains [3] or the Landau-Kovalev-Kondratiuk interacting atomic chains (IAC) model [4]. These models are limited to simplified geometries. In Section 2 of this paper, we describe a more general discrete model of dislocation dynamics in cubic crystals that yields the usual equations of linear anisotropic elasticity far from dislocation cores. In Section 3 we show that moving dislocations can be considered to be traveling waves of discrete model equations and analyze dislocation depinning and motion as an applied stress surpasses Peierls's.

2 DISCRETE MODEL FOR CUBIC CRYSTALS

Let us consider a simple cubic crystal with one atom per lattice point and having a unit cell of side length a. Extensions to face centered cubic and body centered cubic crystals can be found in [5] and to cubic crystals with a two-atom basis in [6]. To find the equations describing our model of dislocation dynamics we proceed as follows. We discretize space along the primitive vectors defining the unit cell of the crystal: $x = x_1 = (l + \epsilon_1)\, a$, $y = x_2 = (m + \epsilon_2)\, a$, $z = x_3 = (n + \epsilon_3)\, a$, where l, m and n are integer numbers. The numbers $\epsilon_i \in (0, 1)$ are chosen different from zero so as to avoid that any lattice site coincide with the origin $x_i = 0$. For a simple cubic crystal it is convenient to set $\epsilon_i = 1/2$, so that the origin is at the center of a unit cell. The discrete displacement vector from lattice sites $u_i(l, m, n; t)$ is a nondimensional vector such that the usual displacement vector $\tilde{u}_i(x, y, z, t)$ becomes $\tilde{u}_i(la, ma, na, t) = a\, u_i(l, m, n; t)$. The *discrete* distortion tensor is defined as

$$w_i^{(j)} = g(D_j^+ u_i), \tag{1}$$

where $g(x)$ is an odd periodic function of period one satisfying $g(x) \sim x$ as $x \to 0$, and D_j^+ and D_j^- represent the standard forward and backward difference operators, so that $D_1^{\pm} u_i(l,m,n;t) = \pm [u_i(l \pm 1, m, n; t) - u_i(l,m,n;t)]$, and so on. $g(x)$ is chosen so that the Peierls stress calculated using the model agrees with experimentally measured values or with results of molecular dynamics simulations [5]. The discrete strain energy is defined by

$$W(\{u_i\})(l,m,n;t) = \frac{a^3}{2} \sum_{i,j,k,l} \sum_{l,m,n} c_{ijkl} e_{ij} e_{kl}, \tag{2}$$

where $e_{ij} = (w_i^{(j)} + w_j^{(i)})/2$ is the discrete strain. Then the Euler-Lagrange equations for the potential energy $V = W + a^3 \sum_{l,m,n} f_i u_i$ (where f_i is related to the body force $\tilde{f}_i$ by $f_i = a\, \tilde{f}_i$) yield the following equations of motion:

$$M\, \ddot{u}_i = \sum_{j,k,l} D_j^- [c_{ijkl}\, g'(D_j^+ u_i)\, g(D_l^+ u_k)] + f_i. \tag{3}$$

Here $\ddot{u}_i \equiv \partial^2 u_i / \partial t^2$, $M = \rho a^2$ has units of mass per unit length (provided ρ is the mass density of the crystal) and the displacement vector is dimensionless, so that both sides of Eq. (3) have units of force per unit area. To recover the continuum limit of our discrete model, we restore dimensional units to Eq. (3) and use

$$u_i(l,m,n;t) = \frac{\tilde{u}_i\, ((l+\epsilon_1)\, a, (m+\epsilon_2)\, a, (n+\epsilon_3)\, a; t)}{a}, \tag{4}$$

where $\tilde{f}_i = f_i / a$, then let $a \to 0$, use $M = \rho a^2$ and $g(x) \sim x$ as $x \to 0$. Then the Cauchy equations of linearized anisotropic elasticity are obtained:

$$\rho\, \frac{\partial^2 \tilde{u}_i}{\partial t^2} = \sum_{j,k,l} \frac{\partial}{\partial x_j} \left(c_{ijkl}\, \frac{\partial \tilde{u}_k}{\partial x_l} \right) + \tilde{f}_i, \tag{5}$$

Viscosity and fluctuation effects can be added as explained in Ref. [2].
As an illustration, we shall construct an edge dislocation in an isotropic simple cubic crystal with planar discrete symmetry, so that $(u_1(l,m;t), u_2(l,m;t), 0)$ is independent of $z = na$. Our procedure is:

- Calculate the corresponding singular solution of the static Navier equations of linear elasticity. Use (4) to obtain a time-independent nondimensional displacement vector $(U_1(l,m), U_2(l,m))$ (note that the singularity at $x_i = 0$ does not coincide with any lattice site).
- Use $U_i(l,m)$, $i = 1, 2$, as the boundary condition at the crystal borders ($l = \pm X$, $m = \pm Y$) and also as an initial condition to solve an overdamped discrete model in which $M\gamma \dot{u}_i$ replaces the left hand side of the equations of motion (3):

$$M\gamma\, \dot{u}_i - \sum_{j,k,l} D_j^- [c_{ijkl}\, g'(D_j^+ u_i)\, g(D_l^+ u_k)] = f_i. \tag{6}$$

- The solution of the overdamped equations of motion tends to the stationary dislocation solution of the discrete model as time goes to infinity.

The solution of the static Navier equations corresponding to an edge dislocation under a dimensionless shear stress F equals the corresponding solution under zero stress plus $(Fy, Fx, 0)$. Then we can use as initial and boundary displacement vector in the previous procedure $(U_1 + Fm, U_2 + Fl, 0)$, provided U_i is the displacement vector under zero shear stress. The resulting edge dislocation is depicted in Fig. 1.

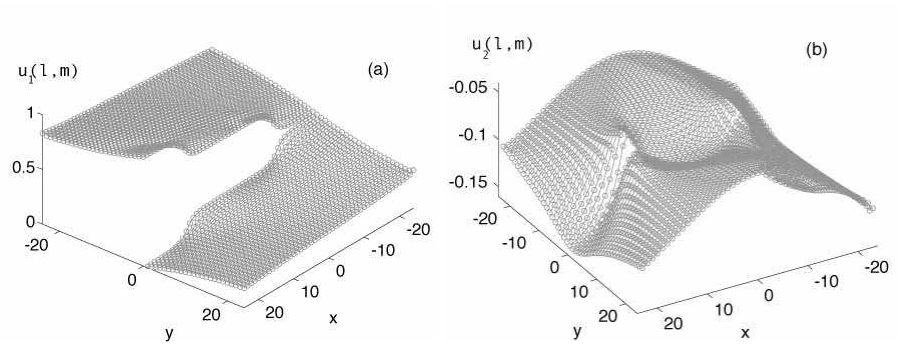

Figure 1: Profile of an edge dislocation for $g(x) = \sin(2\pi x)/(2\pi)$: (a) $u_1(l, m)$, (b) $u_2(l, m)$.

3 DEPINNING OF EDGE DISLOCATIONS

To analyze how dislocations move under a sufficient applied stress, we use a simplified version of Eqs. (3). Planar edge dislocations as in Fig. 1 (with Burgers vector directed along the positive x axis) move from left to right when the applied shear stress parallel to the Burgers vector surpasses Peierls's. The extra half-plane of atoms finishing at the dislocation line glides along the x direction but the atoms do not climb in the y direction. As the dislocation line moves, $D_2^+ u_1$ can be larger than 1 (the period of $g(x)$) but $D_1^+ u_1$ remains always smaller than 1. Therefore, no qualitative features of the model are lost if we set $u_1 = u$, $u_2 = u_3 = 0$, $g'(x) = 1$ (its far field value), and replace $g(D_1^+ u)$ by $D_1^+ u$ in the equations. With these simplifications and for a cubic crystal, Eq. (3) becomes

$$M\ddot{u} + M\gamma\dot{u} = C_{11} D_1^- D_1^+ u + C_{44} D_2^- g(D_2^+ u), \tag{7}$$

in which we have added a damping term in the left hand side and set $f_i = 0$. Using now the notation $u_{i,j}(t)$ instead of $u(i, j; t)$ and the nondimensional time $C_{11}t/(M\gamma) \to t$, defining $\mu = C_{11}/(M\gamma^2)$, $A = C_{44}/C_{11}$ and selecting $g(x) = \sin(2\pi x)/(2\pi)$, we obtain the *nondimensional* equations of the IAC model [4]:

$$\begin{aligned} \mu\,\ddot{u}_{i,j} + \dot{u}_{i,j} &= u_{i+1,j} - 2u_{i,j} + u_{i-1,j} \\ &\quad + A\,\frac{\sin[2\pi(u_{i,j+1} - u_{i,j})] + \sin[2\pi(u_{i,j-1} - u_{i,j})]}{2\pi}. \end{aligned} \tag{8}$$

3.1 Stationary edge dislocation

According to the procedure explained in the previous section, to construct an edge dislocation with Burgers vector $(a, 0)$, we need to obtain the corresponding static solutions of (8) in the continuum limit. These solutions solve $\partial^2\tilde{u}/\partial x^2 + A\,\partial^2\tilde{u}/\partial y^2 = 0$, and satisfy $\oint_c \nabla\tilde{u} \cdot dx = (a, 0)$ for the Burgers circuit around the dislocation line (note that we are using dimensional quantities $\tilde{u} = a\,u$, with $x = ia + 1/2$, $y = ja + 1/2$). Edge dislocations are generated from the zero-stress solution $\tilde{u} = a\,\theta(x, y/\sqrt{A})/(2\pi)$, where $\theta = \tan^{-1}(y/x) \in [0, 2\pi)$ is the angle function. The corresponding strain decays as $1/r$ as $r = \sqrt{x^2 + y^2/A} \to \infty$, same as the elastic strain about an edge dislocation. From the dimensional displacement $\tilde{u}$, we obtain the

discrete static solution:

$$U_{i,j} = \frac{1}{2\pi}\,\theta\left(a\left(i+\frac{1}{2}\right), \frac{a}{\sqrt{A}}\left(j+\frac{1}{2}\right)\right) \equiv \frac{\theta^A_{i,j}}{2\pi}. \tag{9}$$

Under a shear stress F, the static solution is $(jF + \theta^A_{i,j})/(2\pi)$.
Next, we solve numerically Eq. (8) with $\mu = 0$ in a large lattice, using

$$u_{i,j} = \frac{\theta^A_{i,j} + F\,j}{2\pi}, \quad \text{for } i = \pm N \text{ and for } j = \pm N, \text{ and} \quad u_{i,j}(0) = \frac{\theta^A_{i,j}}{2\pi}. \tag{10}$$

If $|F| > F_{\rm cs}(A)$ is large enough ($F_{\rm cs}$ is the *static Peierls stress*), the dislocation is observed to glide in the x direction: to the right if $F > 0$, and to the left if $F < 0$. Provided $|F| < F_{\rm cs}(A)$, the system relaxes to the stationary configuration which we denote by $\hat{U}_{i,j}(F, A)$. The result is quite similar to Fig. 1(a). A theoretical study of these type of solutions, including existence proofs and stability arguments, is given in [8].

3.2 Linear stability analysis of the edge dislocation for $\mu = 0$.

To calculate $F_{\rm cs}(A)$, we perform a linear stability analysis of $\hat{U}(F, A)$. We insert $u_{i,j}(t) = \hat{U}_{i,j}(F, A) + v_{i,j}(t)$ in Eq. (8) with $\mu = 0$ and expand the result in powers of $v_{i,j}$ *about the stationary state* $\hat{U}_{i,j}(A, F)$ keeping up to quadratic terms. Subscripts in the resulting quadratic equation can be numbered with a single one starting from the point $i = j = -N$: $\hat{U}_{i,j} = \hat{U}_k$ and $v_{i,j} = v_k$, $k = i + N + 1 + (j + N)(2N + 1)$ for $i, j = -N, \ldots, N$. The quadratic equation can be written formally as

$$\frac{d\mathbf{v}}{dt} = \mathcal{M}(F)\mathbf{v} + \mathcal{B}(\mathbf{v}, \mathbf{v}; F), \tag{11}$$

where the vector $\mathbf{v}$ has components v_k. The linear stability of the stationary state $\hat{U}_k(A, F)$ depends on the eigenvalues of the matrix $\mathcal{M}(F)$. These eigenvalues are all real negative for $|F| < F_{\rm cs}$ whereas one of them vanishes at $|F| = F_{\rm cs}$ (at this stress, the operator $\mathcal{M}$ in (11) ceases to be elliptic). Fig. 2(a) depicts $F_{\rm cs}$ as a function of A. Since $F_{\rm cs}$ increases with A and the dislocation core decreases with A, narrow core dislocations are harder to move.

3.3 The transition from stationary to moving dislocations as a global bifurcation.

Let us assume that $F > F_{cs}$ (the case $F < -F_{cs}$ is similar). The motion of dislocations depends on whether μ is zero or not. Consider first $\mu = 0$. Let $\mathbf{l}$ and $\mathbf{r}$ (with components l_{ij} and r_{ij}) be the left and right eigenvectors of the matrix $\mathcal{M}(F_{cs})$ corresponding to its zero eigenvalue (its largest one). Then $v_{i,j} = [(F - F_c)j + \phi(t)\, r_{ij}]/(2\pi)$ (plus terms that decay exponentially fast in time) satisfies the BC $v_{i,j} = (F - F_c)j/(2\pi)$ for $j = \pm N$, and $v_{i,j} = 0$ for $i = \pm N$. Inserting $u_{i,j} = \hat{U}_{i,j}(F_{\rm cs}) + v_{i,j}$ in (6) with $\mu = 0$, we obtain

$$\frac{\dot{\phi}}{A} r_{ij} = D_2^- \left[(F - F_{\rm cs})\cos[2\pi(D_2^+ \hat{U}_{i,j})] - \frac{\phi^2 \sin[2\pi(D_2^+ \hat{U}_{i,j})](D_2^+ r_{ij})^2}{2}\right] \tag{12}$$

plus terms of orders $(F - F_{\rm cs})\phi$ and $(F - F_{\rm cs})^2$. The cubic terms that were ignored when (11) was written are of order ϕ^3. The scalar product of this equation by $\mathbf{l}$ yields

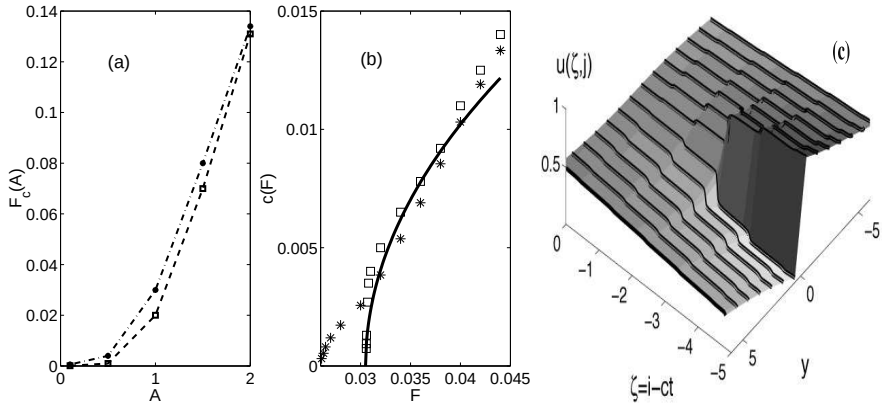

Figure 2: (a) Static (squares, $m = 0$) and dynamic (asterisks, $m = 0.5$) critical stresses F_{cs} and F_{cd} versus A. (b) Theoretical (solid line, $m = 0$) and numerical (squares, $\mu = 0$; asterisks, $\mu = 0.5$) dislocation velocity vs. F ($A = 1$, $N = 25$). (c) Wave front profiles, $u_{i,j}(t) = u(\zeta, j)$, $\zeta = i - ct$, $c > 0$, near $F = F_{cs}$ ($A = 3$, $\mu = 0$, $N = 25$). Adapted from [7]

the following amplitude equation

$$\frac{d\phi}{dt} \quad = \quad \alpha\,(F - F_{\rm cs}) + \beta\phi^2, \tag{13}$$

where $\beta = -A\sum_{ij} l_{ij} D_2^- \{\sin[2\pi(D_2^+ \hat{U}_{i,j})](D_2^+ r_{ij})^2\}/(2\sum_{ij} l_{ij} r_{ij})$ and $\alpha = A\sum_{ij} l_{ij} D_2^- \{\cos[2\pi(D_2^+ \hat{U}_{i,j})]\}/\sum_{ij} l_{ij} r_{ij}$. The two terms in the right hand side of (13) are of order $(F - F_{\rm cs})$, whereby ϕ is of order $(F - F_{\rm cs})^{1/2}$. Then the neglected error terms are of order $(F - F_{\rm cs})^{3/2}$, and they tend faster to zero as $F \to F_{\rm cs}+$ than the terms in (12). Numerical evidence shows that $\alpha > 0$ and $\beta > 0$.
Equation (12) is the normal form of a saddle-node bifurcation. Its solution is

$$\phi(t) = \sqrt{\frac{\alpha\,(F - F_{\rm cs})}{\beta}}\,\tan\left(\sqrt{\alpha\beta\,(F - F_{\rm cs})}\,(t - t_0)\right)\,, \tag{14}$$

which remains close to $\phi = 0$ for long time periods, but it blows up at the large times $(t - t_0) = \pm 1/(2c)$, where $c(A, F) = \pi^{-1}\sqrt{\alpha\beta\,(F - F_{\rm cs})}$.
What happens after the blow up time $(t - t_0) = 1/(2c)$? The approximation $u_{i,j}(t) \sim \hat{U}_{i,j}(F_{\rm cs}, A) + [(F - F_{\rm cs})\,j + \phi(t)\,r_{i,j}]/(2\pi)$ breaks down because $\phi(t)$ is no longer of order $(F - F_{\rm cs})^{1/2}$. We have to solve an inner problem consisting of Equations (8) at $F = F_{\rm cs}$ with the matching conditions $u_{i,j} \sim \hat{U}_{i,j}(F_{\rm cs}, A) + r_{ij}/[\pi^2\sqrt{\beta/[\alpha\,(F - F_c)]} - 2\pi\beta\,(t - t_0)]$, as $(t - t_0) \to -\infty$. This inner solution evolves towards $\hat{U}_{i-1,j}$ in a time of order 1 after $(t - t_0) = 1/(2c)$. Then another jump of the whole dislocation profile to the right occurs when $(t - t_0) = 1/c$, and so on. The dislocation is moving to the right with velocity $c(A, F)$ given above and its profile is $u_{i,j}(t) = u(\zeta, j)$, $\zeta = i - ct$, which has been depicted in Fig. 2(c). Notice that the wave front profiles exhibit many smoothed steps for F slightly larger than $F_{\rm cs}$. In the flat part of these

steps, $u(\zeta, j)$ takes on the stationary values $\hat{U}_{i,j}(F_{\rm cs})$ because $\phi(t)$ in (14) is almost zero for $|c(t-t_0)| < 1/2$. The steep parts of the profiles between steps correspond to the solutions of the inner problem.
Numerically measured and theoretically predicted dislocation velocities are compared in Fig. 2(b). The numerical calculation of the dislocation velocity is somewhat delicate. If we solve numerically the initial-boundary value problem (8) and (10) for $|F| > F_{\rm cs}$, the velocity of the dislocation decreases as it moves towards the boundary. The dislocation decelerates because we are using the far field of a steady dislocation as boundary condition, instead of the (more sensible) far field of a moving dislocation. However, the latter is in principle unknown because we do not know the dislocation speed. We will assume nevertheless that the dislocation moves at constant speed c once it starts moving, as it would in a stressed infinite system. Then the correct dislocation far field is $(\theta^A_{i-ct,j} + Fj)/(2\pi)$. With this far field as boundary condition, Eq. (8) has traveling wave solutions $u_{i,j}(t)$ whose velocity can be calculated self-consistently. How? By an iterative procedure that adopts as initial trial velocity that of a dislocation subject to static boundary condition (10) as it starts moving. Figure 2(b) compares the numerically calculated velocity with the theoretical prediction. As explained above, step-like profiles are observed near threshold (see Fig. 2(c)), that become smoother as F increases. Note that the wave front profiles are kinks for $j < 0$ and antikinks for $j \geq 0$.

3.4 Effects of inertia ($\mu > 0$)

Numerical simulations of (8) with $\mu > 0$ show that the dislocations keep moving for an interval of stresses below the static Peierls stress, $F_{cd} < |F| < F_{cs}$. For these stresses, stable solutions representing static and moving dislocations coexist: to depin a static dislocation, we need $|F| > F_{cs}$. However if $|F|$ decreases below F_{cs}, a moving dislocation keeps moving until $|F| < F_{cd}$; see Fig. 2(b). Thus F_{cd} represents the *dynamic Peierls stress* of the dislocation. Our theory therefore yields the static and the dynamic Peierls stresses and the velocity of a dislocation.

Acknowledgments

Work financed by the MEC grants MAT2005-05730-C02-01 and 02.

References

[1] J. Frenkel and T. Kontorova. On the theory of plastic deformation and twinning. *J. Phys. Moscow* 1:137–149, 1939.

[2] J.P. Hirth and J. Lothe. *Theory of Dislocations*, 2nd ed. Wiley,1982.

[3] H. Suzuki. Motion of dislocations in body-centered cubic crystals. In A. H. Rosenfield et al, editors, *Dislocation Dynamics*, pages 679–700. MacGraw Hill, 1967.

[4] A. I. Landau, A.S. Kovalev and A. D. Kondratyuk. Model of interacting atomic chains and its application to the description of the crowdion in an anisotropic crystal. *Phys. stat. sol. (b)* 179:373–381, 1993.

[5] A. Carpio and L. L. Bonilla. Discrete models of dislocations and their motion in cubic crystals. *Physical Review B* 71:134105, 2005.

[6] L.L. Bonilla, A. Carpio and I. Plans. Dislocations in cubic crystals described by discrete models. *Physica A* 376:361–377, 2007.

[7] A. Carpio and L.L. Bonilla. Edge dislocations in crystal structures considered as traveling waves of discrete models. *Physical Review Letters* 90: 135502, 2003.

[8] A. Carpio. Wavefronts for discrete two-dimensional nonlinear diffusion equations. *Applied Mathematics Letters* 15: 415–421, 2002.